# Four-lepton $Z$ boson decay constraints on the standard model EFT

Radja Boughezal,[1] Chien-Yi Chen,[2] Frank Petriello,[1,2] and Daniel Wiegand[1,2]
[1]*HEP Division, Argonne National Laboratory, Argonne, Illinois 60439, USA*
[2]*Department of Physics & Astronomy, Northwestern University, Evanston, Illinois 60208, USA*

(Received 20 October 2020; accepted 2 March 2021; published 19 March 2021)

We discuss how four-lepton decays of the $Z$ boson probe currently unconstrained flat directions in the parameter space of the standard model effective field theory (SMEFT). We derive the constraints from these decays on four-lepton operators in the SMEFT and show how the LHC data for this process complements probes from neutrino-trident production. Future differential measurements with high-luminosity data can strongly constrain four-lepton operators and remove all flat directions in the four-muon sector of the SMEFT. We comment briefly on the possibility of using rare $Z$-decays to $\tau$-leptons to probe untested directions in the SMEFT parameter space.

DOI: 10.1103/PhysRevD.103.055015

## I. INTRODUCTION

The search for physics beyond the Standard Model (SM) at the Large Hadron Collider (LHC) and other experiments has so far yielded no new particles. This lack of evidence for new electroweak-scale physics suggests that there is a mass gap between the SM and the next energy scale at which new particles appear. Although the search for new particles will continue in the future at the high-luminosity LHC, it is becoming increasingly important to search for potentially small and subtle indirect signatures of new physics, and to understand the constraints imposed by current data on high-scale new physics. A systematic framework for characterizing deviations from the SM in the presence of no new electroweak-scale particle is the SM effective field theory (SMEFT). The SMEFT is constructed by allowing higher-dimensional operators containing only SM fields that respect the SM gauge symmetries. These operators are suppressed by an energy scale $\Lambda$ at which the effective theory breaks down and new fields must be added to the Lagrangian. The leading lepton-number conserving dimension-6 operators characterizing deviations from the SM have been classified [1–3].

Significant effort has been devoted to performing global analyses of the available data within the SMEFT framework with varying assumptions [4–18]. Since the general dimension-6 SMEFT Lagrangian contains 2499 parameters for three generations assuming baryon-number conservation, quite often additional flavor symmetries such as minimal flavor violation (MFV) are assumed in order to reduce the number of Wilson coefficients. Assuming MFV implies that the flavor structure of the SMEFT Wilson coefficients are carried by combinations of Yukawa matrices. This leads to several familiar intuitions [19,20]: for example, that the coefficients of scalar and dipole operators are suppressed by small fermion masses for the lighter generations, and that vector four-fermion interactions are generation-independent. Flavor assumptions such as MFV lead to several advantages. In general fits without such flavor assumptions, flat directions exist since current experimental constraints cannot access all possible Wilson coefficients. MFV also effectively suppresses strongly constrained flavor-violating effects.

Despite these advantages it remains important to extend fits within the SMEFT framework beyond the MFV assumption. Going beyond MFV allows global fits to encompass a broader range of ultraviolet completions. For example, models which attempt to explain discrepancies in rare $B$-meson decays have a structure that violates lepton flavor universality [21]. Allowing for flavor structure in the SMEFT requires addressing and removing the flat directions between Wilson coefficients that appear. The removal of flat directions in fits to SMEFT Wilson coefficients require the use of additional processes and experiments [22]. In this work we point out that the rare $Z$ boson decays to four-leptons offer the potential to probe combinations of four-fermion Wilson coefficients not accessible in other measurements. In particular, only a single combination of four-muon Wilson coefficients is currently constrained in global fits by the neutrino-trident production process $\gamma^* \nu_\mu \to \nu_\mu \mu^+ \mu^-$ [13,23]. Four-muon $Z$ boson decays at the LHC probe orthogonal combinations of these Wilson coefficients, allowing for a complete determination of the four-muon operators in the SMEFT.

*Published by the American Physical Society under the terms of the Creative Commons Attribution 4.0 International license. Further distribution of this work must maintain attribution to the author(s) and the published article's title, journal citation, and DOI. Funded by SCOAP³.*

The potential of four-lepton decay modes to constrain physics beyond the SM has been investigated previously, particularly in the context of $Z'$ models [23,24]. We study the constraints imposed by current LHC data, as well as potential future constraints at a high-luminosity LHC. Current measurements of this mode consider only the total rate. We point out that differential measurements can completely determine all four-muon Wilson coefficients, which motivates their study with future high-luminosity data. Although we focus here on the four-muon mode as experimental searches for $Z \to 4\mu$ exist, other channels such as $Z \to 2\tau 2\mu$ and $Z \to 4\tau$ may provide probes of completely untested parameters in the SMEFT. We comment briefly on this possibility in our conclusions.

Our paper is organized as follows. We review aspects of the SMEFT needed for our analysis in Sec. II. In Sec. III we study the constraints imposed by inclusive LHC measurements of the $Z \to 4\mu$ decay rate on the SMEFT four-muon operators. We also discuss their complementarity with constraints from neutrino-trident production. We discuss what can be learned from future differential LHC measurements in Sec. IV. Finally, we conclude in Sec. V.

## II. REVIEW OF THE SMEFT

We review in this section aspects of the SMEFT relevant for our analysis of four-muon decays of the $Z$ boson. The SMEFT is an extension of the SM Lagrangian to include terms suppressed by an energy scale $\Lambda$ at which the ultraviolet completion becomes important and new particles beyond the SM appear. Truncating the expansion in $1/\Lambda$ at dimension-6, and ignoring operators of odd-dimension which violate lepton number, we have

$$\mathcal{L} = \mathcal{L}_{\rm SM} + \frac{1}{\Lambda^2}\sum_i C_i \mathcal{O}_i + \cdots, \tag{1}$$

where the ellipsis denotes operators of higher dimensions. The Wilson coefficients $C_i$ defined above are dimensionless. When computing the $Z$ boson decay width we consider only the leading interference of the SM amplitude with the dimension-6 contribution. This is consistent with our truncation of the SMEFT expansion above, since the dimension-6 squared contributions are formally the same order in the $1/\Lambda$ expansion as the dimension-8 terms which we neglect. The Wilson coefficients are renormalization-scheme dependent quantities. In an $\overline{\rm MS}$ scheme they become scale-dependent and run with energy. As we perform only a leading-order analysis in this manuscript we neglect this running.

Corrections to the $Z \to 4l$ decay widths come from two sources: shifts of the $Z\bar{l}l$ and $\gamma\bar{l}l$ vertices that scale as $v^2/\Lambda^2$ where $v$ is the Higgs vev, and four-fermion operators which scale as $E^2/\Lambda^2$ where $E$ is the characteristic energy scale of the process. Note that the $\gamma\bar{l}l$ vertex is shifted from the SM expression in the $(G_\mu, M_W, M_Z)$ input parameter scheme [25] adopted here since the electromagnetic coupling is shifted. We summarize in Table I the dimension-6 operators that shift the decay width at leading-order in its perturbative expansion. Here, $l$ denotes a Dirac lepton, $\phi$ the Higgs boson, and $W$ and $B$ the field-strength tensors of the $\mathrm{SU}(3) \times \mathrm{U}(1)$ gauge bosons. $p, r, s, t$ denote generation indices. We have introduced explicit projection operators $P_{L,R}$ to denote the projections onto left-handed doublets and right-handed singlets. All operators containing the Higgs field $\phi$ only shift the $Z\bar{l}l$ and $\gamma\bar{l}l$ vertices and can be combined into shift constants $\delta g_Z^L$, $\delta g_Z^R$, $\delta g_\gamma^L$ and $\delta g_\gamma^R$ respectively. We note that $\delta g_\gamma^R = \delta g_\gamma^L = \delta g_\gamma$. Explicit expressions for these shifts are given in Appendix A.

TABLE I. Dimension-6 operators contributing to the decay $Z \to 4l$. The last five operators only lead to overall shifts of the SM $Z\bar{l}l$ and $\gamma\bar{l}l$ vertices.

| | |
|---|---|
| $\mathcal{O}_{\substack{ll \\ prst}}$ | $(\bar{l}_p\gamma^\mu P_L l_r)(\bar{l}_s\gamma_\mu P_L l_t)$ |
| $\mathcal{O}_{\substack{ee \\ prst}}$ | $(\bar{l}_p\gamma^\mu P_R l_r)(\bar{l}_s\gamma_\mu P_R l_t)$ |
| $\mathcal{O}_{\phi D}$ | $(\phi^\dagger D^\mu \phi)^*(\phi^\dagger D_\mu \phi)$ |
| $\mathcal{O}^{(1)}_{\substack{\phi l \\ rs}}$ | $i(\phi^\dagger \overleftrightarrow{D}_\mu \phi)(\bar{l}_r\gamma^\mu P_L l_s)$ |
| $\mathcal{O}_{\substack{le \\ prst}}$ | $(\bar{l}_p\gamma^\mu P_L l_r)(\bar{l}_s\gamma_\mu P_R l_t)$ |
| $\mathcal{O}_{\phi W B}$ | $\phi^\dagger \tau^I \phi W^I_{\mu\nu} B^{\mu\nu}$ |
| $\mathcal{O}_{\substack{\phi e \\ rs}}$ | $i(\phi^\dagger \overleftrightarrow{D}_\mu \phi)(\bar{l}_r\gamma^\mu P_R l_s)$ |
| $\mathcal{O}^{(3)}_{\substack{\phi l \\ rs}}$ | $i(\phi^\dagger \overleftrightarrow{D}^I_\mu \phi)(\bar{l}_r\tau^I\gamma^\mu P_L l_s)$ |

There are potentially additional dimension-6 contributions from operators modifying the total $Z$ boson decay width that appear in the denominator of the branching ratio. To study these effects we express each $Z$ boson partial width in terms of its dimension-4 and dimension-6 contribution:

$$\Gamma_i = \Gamma_i^{(4)} + \Gamma_i^{(6)}, \tag{2}$$

where the dimension-6 contribution is assumed to be small. The branching ratio for $Z \to 4\mu$ can then be written as

$$\mathrm{BR}(Z \to 4\mu) = \frac{\Gamma(Z \to 4\mu)}{\sum_i \Gamma_i} \approx \frac{\Gamma^{(4)}(Z \to 4\mu)}{\sum_i \Gamma_i^{(4)}} \times \left[1 + \frac{\Gamma^{(6)}(Z \to 4\mu)}{\Gamma^{(4)}(Z \to 4\mu)} - \frac{\sum_i \Gamma_i^{(6)}}{\sum_i \Gamma_i^{(4)}}\right] \tag{3}$$

where the sum over $i$ includes all $Z$ boson decay modes and we have expanded to linear order in the dimension-6 corrections. The second term in the square bracket above comes from the dimension-6 corrections to the total decay width. Since $\sum_i \Gamma_i^{(4)} \gg \Gamma^{(4)}(Z \to 4\mu)$, the only significant corrections from this last term come from the large $Z$ partial decay widths. We assume that the dominant corrections

TABLE II. Results for the $a_i$ coefficients given the cuts 80 GeV $< m_{4l} <$ 100 GeV and $m_{ll} > 4$ GeV. For comparison with the available $Z$-pole bounds we assume flavor universality for the vertex-shift operators.

| $a_{ll}$ | $a_{ee}$ | $a_{le}$ | $a^L_{Zl}$ | $a^R_{Zl}$ | $a_{\gamma\mu}$ | $a^L_{Z\nu}$ | $a^L_{Zu}$ | $a^R_{Zu}$ | $a^L_{Zd}$ | $a^R_{Zd}$ |
|---|---|---|---|---|---|---|---|---|---|---|
| 0.025 | 0.016 | 0.009 | 4.2 | −3.3 | 4.0 | −0.40 | −0.39 | −0.071 | −0.87 | −0.027 |

come from the $Z \to \bar{f}f$ decay widths. The corrections to these widths come from shifts in the left and right-handed couplings of the $Z$ boson to the different fermions, and are analogous to the operators leading to the shifts of the leptonic vertices in Table I above. We will study the effects from shifts to the $Z \to \bar{f}f$ decays and absorb them into global shift factors $\delta g^{L,R}_{Zf}$ for each fermion species.

Finally, we note that dipole operators that can potentially contribute vanish for massless fermions upon truncation of the EFT expansion to dimension-6, which we assume here. The explicit expressions for all decay widths in terms of the SMEFT coefficients can be found in Appendix A.

## III. CONSTRAINING THE FOUR-LEPTON OPERATORS

The coefficients parameterizing the SMEFT contributions to the decay $Z \to 4\mu$ depend on the matrix elements describing the process and the imposed experimental cuts. We evaluate them numerically at leading-order using the MADGRAPH package SMEFTsim [25]. The UV scale $\Lambda$ is set to the Higgs vacuum expectation value $v = 246$ GeV for comparison with previous results in the literature [13]. Explicit expressions for the four-lepton decay widths are given in Appendix B. We express the deviation for the four-muon decay mode in terms of the normalized branching ratio:

$$\frac{\mathrm{BR}(Z \to 4\mu)}{\mathrm{BR}_{\mathrm{SM}}} = 1 + a_{ll} C_{\substack{ll \\ 2222}} + a_{le} C_{\substack{le \\ 2222}} + a_{ee} C_{\substack{ee \\ 2222}} + a^L_{Zl}\delta g^L_{Zl} + a^R_{Zl}\delta g^R_{Zl} + a_{\gamma\mu}\delta g_{\gamma\mu} + a^L_{Z\nu}\delta g^L_{Z\nu} + a^L_{Zu}\delta g^L_{Zu} + a^R_{Zu}\delta g^R_{Zu} + a^L_{d}\delta g^L_{Zd} + a^R_{d}\delta g^R_{Zd}, \quad (4)$$

where we assume lepton and quark flavor universality for the vertex shift operators for clarity of this argument. We note from the expression above that this decay is directly sensitive to the four-muon couplings in the SMEFT, making it of interest for accessing these operators.

We discuss next how well measurements of the inclusive $Z \to 4\mu$ decay width can constrain the four-muon SMEFT operators defined in the previous section. We first show that after accounting for the strong constraints on the vertex shifts from $Z \to 2f$ decays at LEP and other experiments, measurements of the $Z \to 4l$ decay are primarily sensitive to leptonic four-fermion operators, which are not as strongly bounded yet. The relevant comparison to establish whether $Z$ vertex shifts or four-fermion terms dominate the SMEFT correction is the size of $a_i C_i$ for each term defined in Eq. (4). We evaluate the branching ratio imposing 80 GeV $< m_{4l} <$ 100 GeV and $m_{ll} > 4$ GeV for all fermion pairs, consistent with experimental analyses, and obtain the results for the $a_i$ shown in Table II. The lepton vertex-shift $a^{L,R}_{Zl}$ factors are in general two orders of magnitude larger than the four-muon $a$ coefficients for the relevant experimental cuts. However, the $\delta g^{L,R}_{Zl}$ are strongly constrained by Z-pole data. After accounting for these constraints the allowed deviations on the $Z \to 4\mu$ branching ratio from vertex shifts are negligibly small. To demonstrate this we begin with the bounds on the SMEFT Wilson coefficients from $Z$-pole data, taken from [26], where flavor universality is assumed and $\Lambda = 246$ GeV. These are summarized in Table III. We then use the formulae compiled in Appendix A to translate these Wilson coefficient bounds into allowed shifts of the leptonic $Zll$ and $\gamma ll$ vertices:

$$|\delta g^L_{Zl}| < 0.0025, \quad |\delta g^R_{Zl}| < 0.0050, \quad |\delta g_{\gamma l}| < 0.0036. \quad (5)$$

The largest of these effects leads to a shift in $\mathrm{BR}(Z \to 4\mu)$ of 1%, which is far smaller than the deviation allowed by the experimental bound and also much smaller than any effect we consider arising from four-fermion interactions. The hadronic vertex shifts that enter the branching fraction through the total width are similarly constrained by the available LEP data. Following the same procedure as the leptonic case we find the constraints:

TABLE III. 68% confidence-level (C.L.) bounds for a single Wilson coefficient fron $Z$-pole data. The UV scale is set to $\Lambda = 246$ GeV. The bounds are derived assuming flavor universality. These numbers are taken from Ref. [26].

| | |
|---|---|
| $\lvert C_{\phi D}\rvert$ | <0.0012 |
| $\lvert C_{\phi WB}\rvert$ | <0.0017 |
| $\lvert C_{ll}\rvert$ | <0.0006 |
| $\lvert C^{(1)}_{\phi q}\rvert$ | <0.0023 |
| $\lvert C_{\phi u}\rvert$ | <0.0073 |
| $\lvert C^{(1)}_{\phi l}\rvert$ | <0.0006 |
| $\lvert C^{(3)}_{\phi l}\rvert$ | <0.0029 |
| $\lvert C_{\phi e}\rvert$ | <0.0003 |
| $\lvert C^{(3)}_{\phi q}\rvert$ | <0.0005 |
| $\lvert C_{\phi d}\rvert$ | <0.014 |

$$|\delta g^L_{Zu}| < 0.0047, \qquad |\delta g^R_{Zu}| < 0.0250,$$
$$|\delta g^L_{Zd}| < 0.0041, \qquad |\delta g^R_{Zd}| < 0.0943. \tag{6}$$

The shift factors $a^{L,R}_{Zu,d}$ are small, and these corrections lead to even smaller effects on $\mathrm{BR}(Z \to 4\mu)$ than in the leptonic case. This shows that the effects of vertex shifts can be safely neglected in our analysis, and we do so in what follows.

### A. Single Wilson-coefficient constraints from inclusive LHC measurements

Both ATLAS and CMS have performed measurements of the $Z \to 4l$ branching ratios [27–30]. These experiments are summarized in Ref. [24], where a combination of existing results is also given. The combined measurement of the $Z \to 4l$ branching ratio is

$$\mathrm{BR}(Z \to 4l) = (4.58 \pm 0.26) \times 10^{-6}. \tag{7}$$

The measurements are scaled via a Monte-Carlo simulation to the following common phase-space region:

$$80\ \mathrm{GeV} < m_{4l} < 100\ \mathrm{GeV}, \qquad m_{l^+l^-} > 4\ \mathrm{GeV} \tag{8}$$

where $m_{l^+l^-}$ refers to the invariant mass of any combination of oppositely charged leptons. As our interest is in the four-muon mode, we convert this combination to a result for $\mathrm{BR}(Z \to 4\mu)$ as follows. For each of the experimental measurements in Table 1 of Ref. [24] we scale the central value by the leading-order ratio $\Gamma(Z \to 4\mu)/\Gamma(Z \to 4l)$ computed using MADGRAPH, and the statistical uncertainty by $\sqrt{\Gamma(Z \to 4l)/\Gamma(Z \to 4\mu)}$. Combining the results yields

$$\mathrm{BR}(Z \to 4\mu) = (1.21 \pm 0.41) \times 10^{-6}. \tag{9}$$

We have checked that including the correlation coefficients listed in Table 2 of Ref. [24] does not significantly change this result. We estimate the expected constraints from an inclusive measurement at a high-luminosity LHC by assuming that both statistical and systematic errors scale as $1/\sqrt{\mathcal{L}}$, where $\mathcal{L}$ is the integrated luminosity. We show the current constraints and those from a HL-LHC assuming 3000 $\mathrm{fb}^{-1}$ below in Table IV for each four-muon Wilson coefficient turned on separately. The current constraints on the Wilson coefficients from the inclusive branching ratio measurement are quite weak. They become much stronger with the full HL-LHC dataset. We note that the choice of the phase-space constraint $m_{l^+l^-}$ was not optimized for SMEFT studies. However, the effect of increasing this cut does not lead to stronger constraints with the current LHC data. We estimate this by using MADGRAPH to compute the change in branching ratio and consequently statistical error that occurs by increasing the cut on $m_{l^+l^-}$. Although increasing the cut increases the size of the SMEFT-induced deviation since it grows with energy, the corresponding increase in the statistical error overwhelms this growth and leads to weaker bounds.

TABLE IV. Single parameter constraints on the Wilson coefficients of the four-$\mu$ operators at 68% CL for both the current LHC data and a projection based on the HL-LHC with a luminosity of 3 $\mathrm{ab}^{-1}$. For the projection of the uncertainties at the HL-LHC, we assume that all uncertainties scale as $\frac{1}{\sqrt{N}}$.

| | Current ($Z \to 4\mu$) | HL-LHC ($Z \to 4\mu$) |
|---|---|---|
| $\lvert C^{ll}_{2222}\rvert$ | <10.5 | <1.0 |
| $\lvert C^{ee}_{2222}\rvert$ | <16.9 | <1.6 |
| $\lvert C^{le}_{2222}\rvert$ | <28.8 | <2.7 |

### B. Complementarity with neutrino trident production

Another constraint on four-muon operators comes from the neutrino-trident production process $\nu_\mu \gamma^* \to \nu_\mu \mu^+ \mu^-$ which occurs in the Coulomb field of a heavy nucleus. Formulas for the deviation of this process from SM predictions within the SMEFT framework are given in Ref. [13]. We reproduce this deviation below:

$$\frac{\sigma_{\mathrm{trident}}}{\sigma^{\mathrm{SM}}_{\mathrm{trident}}} = 1 + \frac{2}{(1 + 4s^2_W + 8s^4_W)} \frac{v^2}{\Lambda^2} \times \{(C^{ll}_{1221} - C^{ll}_{2222})(1 + 2s^2_W) - 2s^2_W C^{le}_{2222} + 2(\delta g^L_{W\mu} + \delta g^L_{Z\mu} - \delta g^L_{Z\nu_\mu} + 2s^2_W \delta g^L_{W\mu} + 2\delta g^L_{Z\mu} s^2_W + 2s^2_W \delta g^R_{Z\mu} + 8s^4_W \delta g^L_{Z\nu_\mu} - (1 + 2s^2_W)\delta g^L_{We})\} \tag{10}$$

where $\delta g^L_{W\mu}$ is the shift to the $W\mu\nu_\mu$ vertex. Its explicit expression in terms of standard SMEFT operators is given in Appendix A. We see that the deviation depends on the following combination of four-muon Wilson coefficients:

$$\hat{C}^{2222}_{ll} = C^{ll}_{2222} + \frac{2s^2_W}{1 + 2s^2_W} C^{le}_{2222}. \tag{11}$$

From this we see that this measurement is proportional to only a single combination of $C^{ll}_{2222}$ and $C^{le}_{2222}$, and is insensitive to $C^{ee}_{2222}$. The $Z \to 4\mu$ decay is sensitive to all three operators in a different combination than neutrino-trident production. Once differential measurements are made with higher luminosities, all three four-muon Wilson coefficients can be separately determined from a combination of neutrino-trident production and LHC data.

To demonstrate what can be learned from a combination of neutrino-trident production and inclusive $Z \to 4\mu$ measurements at the LHC we perform fits to the inclusive LHC measurement and neutrino-trident production data from the

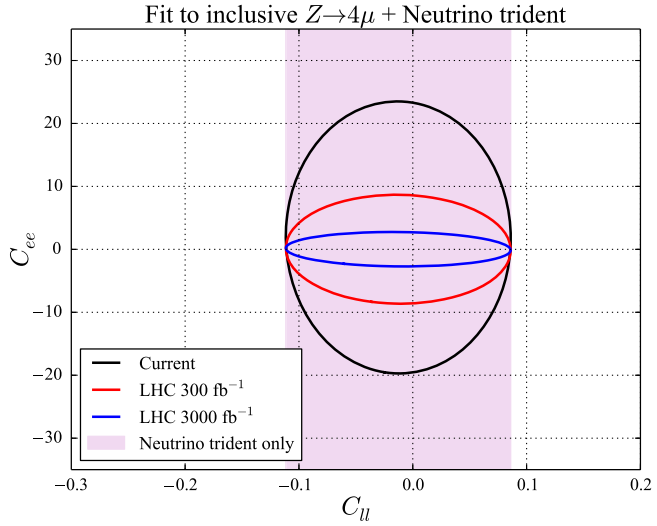


FIG. 1. 68% C.L. bounds on the combination of inclusive LHC $Z \to 4\mu$ data and neutrino trident production assuming nonzero $C_{\substack{ll\\2222}}$ and $C_{\substack{ee\\2222}}$

experiments CCFR [31] and CHARM-II [32]. We consider two different choices of Wilson coefficients:

(1) $C_{\substack{ll\\2222}}$ and $C_{\substack{ee\\2222}}$ nonzero;
(2) $C_{\substack{le\\2222}}$ and $C_{\substack{ee\\2222}}$ nonzero.

The results of these fits are shown in Figs. 1 and 2. The solid bands refer to the constraints from neutrino trident production. We see that this data is not sensitive to $C_{\substack{ee\\2222}}$. The ellipses refer to current LHC constraints, and projections for 300 fb$^{-1}$ and 3000 fb$^{-1}$ of integrated luminosity. Including the LHC data removes the flat direction that occurs due to the insensitivity of neutrino-trident production to $C_{\substack{ee\\2222}}$. We note that the constraints from neutrino

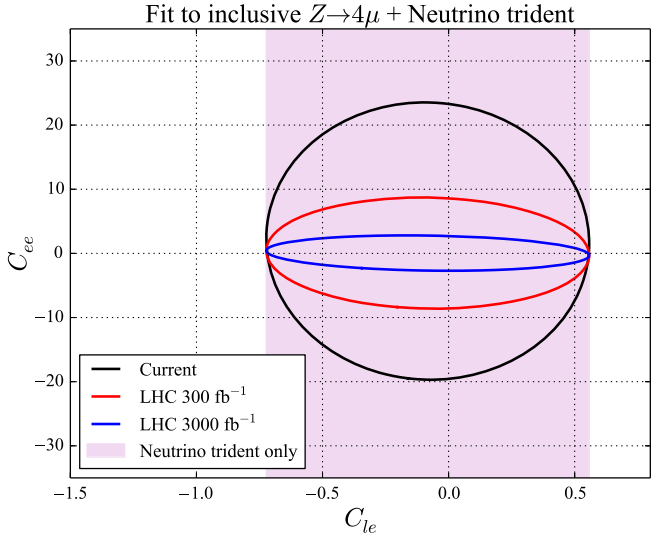


FIG. 2. 68% C.L. bounds on the combination of inclusive LHC $Z \to 4\mu$ data and neutrino trident production assuming nonzero $C_{\substack{le\\2222}}$ and $C_{\substack{ee\\2222}}$

trident production on $C_{\substack{ll\\2222}}$ and $C_{\substack{le\\2222}}$ are stronger than the current LHC bounds, with these coefficients constrained to be less than unity while current LHC data only requires $C_{\substack{ee\\2222}} \lesssim 20$. The power of the LHC measurement increases with higher luminosities. With 3000 fb$^{-1}$ the constraints on $C_{\substack{ee\\2222}}$ approach the level of the neutrino-trident production bounds on $C_{\substack{ll\\2222}}$ and $C_{\substack{le\\2222}}$.

## IV. DIFFERENTIAL MEASUREMENTS WITH FUTURE LHC DATA

The fits in the previous section to the inclusive $Z \to 4\mu$ measurement and neutrino-trident production probe two independent combinations of the three four-muon Wilson coefficients. With differential measurements of $Z \to 4\mu$, all three coefficients can be determined. Enough $Z \to 4\mu$ events will be available to allow for differential measurements with high-luminosity LHC data. Four-lepton final states are defined by five angles [33]: $\theta_1$, $\theta_2$, $\theta^*$, $\Phi_1$, and $\Phi$. We illustrate their definitions in Fig. 3. When defining these angles we have several choices of pairing each muon with an antimuon. Labeling the muon momenta as $p_1$, $p_2$ with $p_T(p_1) > p_T(p_2)$, and the antimuons as $p_3$, $p_4$ with $p_T(p_3) > p_T(p_4)$, we find that if we look at single-differential distributions, the pairing that gives the most discrimination between SMEFT-induced deviations and the SM is $p_1$ with $p_4$ and $p_2$ with $p_3$. To demonstrate that this is the optimal pairing we perform simple one-dimensional fits between the SM and the SMEFT with a single Wilson coefficient turned on. We define the following test statistic:

$$\chi^2 \equiv \sum_{i=1}^{\#\text{of bins}} \frac{(N_i^{\text{SMEFT}} - N_i^{\text{SM}})^2}{(\sigma_i^{\text{SM}})^2} \tag{12}$$

where the number of bins is set to 10 and $N_i^{\text{SM}}(N_i^{\text{SMEFT}})$ stands for the number of SM (SMEFT) events in the $i$th bin. $\sigma_i^{\text{SM}} = \sqrt{N_i^{\text{SM}}}$ represents the standard deviation of the $i$th

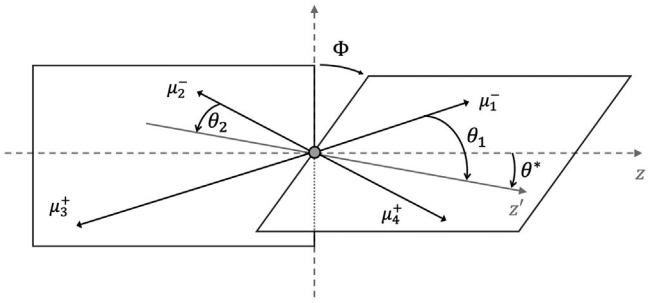


FIG. 3. Illustration of the angles characterizing the decay $Z \to 4\mu$ in the rest frame of the $Z$ boson. The nomenclature is adapted from [33]. $Z'$ denotes the direction of the boost of the highest $p_T$ muon-system. Not shown is the angle $\Phi_1$ which is between the normal vectors of the planes spanned by the $Z$ axis and $Z'$ as well as the one spanned by the highest $p_T$ muons.

TABLE V. $\chi^2$ values for the five single-differential distribution. $l_1$ and $l_3$ ($l_2$ and $l_4$) are grouped together in the same decay plane. The three largest $\chi^2$ values are highlighted.

| $(l_1, l_3)$ | $\cos\theta^*$ | $\cos\theta_1$ | $\cos\theta_2$ | $\Phi_1$ | $\Phi$ |
|---|---|---|---|---|---|
| $C_{\substack{ll \\ 2222}}$ | 39.8 | 73.3 | 18.1 | 9.7 | 15.2 |
| $C_{\substack{ee \\ 2222}}$ | 37.3 | 41.6 | 14.0 | 17.0 | 16.9 |
| $C_{\substack{le \\ 2222}}$ | 16.0 | 51.0 | 18.7 | 10.2 | 76.3 |

bin. For each of the four-muon Wilson coefficients we use this test statistic to probe the sensitivity of each variable to deviations for each pairing. The results are shown in Tables V and VI, where we have highlighted the three most discriminating cases for each pairing. We see that the $p_1 - p_4$ pairing is generally more sensitive, and that the most discriminating variables are $\theta_1$ and $\theta_2$.

To determine the sensitivity of the future LHC data to four-muon Wilson coefficients, and its complementarity with neutrino-trident production, we perform fits to both datasets. We study both 300 fb$^{-1}$ and 3000 fb$^{-1}$ to mimic future LHC datasets. We construct a two-dimensional differential distribution based on the variables $\theta_1$ and $\theta_2$, which were found above to be the most sensitive to SMEFT-induced deviations. While a more sophisticated multi-variate analysis could potentially improve the results found here, we believe that our approach captures the essence of what can be learned from differential measurements. We define a $\chi^2$ function as follows:

$$\chi^2 \equiv \sum_{i=\#\text{ of bins}} \frac{(N_i^{\text{theo}} - N_i^{\text{exp}})^2}{(\sigma_i^{\text{exp}})^2} + \sum_j \frac{(f_j^{\text{theo}} - f_j^{\text{exp}})^2}{(\sigma_j^{\text{exp}})^2} \qquad (13)$$

where the first term accounts for predicted future LHC data for $Z \to 4\mu$. $i$ ranges from 1 to the number of bins of a given differential distribution. In constructing our binning we impose the requirement $N_i > 10$ so that we can assume Gaussian errors. The cuts used in Ref. [29] are applied. We conservatively use the systematic uncertainty from Ref. [29], neglecting possible improvements with future LHC data, and assume that it is constant and uncorrelated for all bins. We stress that this is only a simple estimate of the LHC potential, and is meant to motivate more detailed future experimental studies. The statistical uncertainty of the $i$th bin is assumed to be $\sqrt{N_i}$. The second term in Eq. (13) accounts for the neutrino-trident experimental measurements discussed in Section III B. $f_j^{\text{theo}}$ denotes the theoretical prediction for the neutrino-trident cross section given in Eq. (10), while the $f_j^{\text{exp}}$ are the experimental measurements from CCFR and CHARM-II. The $\sigma_j^{\text{exp}}$ in the denominator denote the experimental errors.

TABLE VI. $\chi^2$ values for the five single-differential distribution. $l_1$ and $l_4$ ($l_2$ and $l_3$) are grouped together in the same decay plane here. The three largest $\chi^2$ values are highlighted.

| $(l_1, l_4)$ | $\cos\theta^*$ | $\cos\theta_1$ | $\cos\theta_2$ | $\Phi_1$ | $\Phi$ |
|---|---|---|---|---|---|
| $C_{\substack{ll \\ 2222}}$ | 24.6 | 77.8 | 61.6 | 24.1 | 65.3 |
| $C_{\substack{2222 \\ 22}}$ | 11.6 | 44.9 | 102.1 | 21.0 | 69.6 |
| $C_{\substack{le \\ 2222}}$ | 6.6 | 375.2 | 335.5 | 25.5 | 48.7 |

To permit simple two-dimensional representations of our results we allow $C_{\substack{ll \\ 2222}}$ and $C_{\substack{le \\ 2222}}$ to be non-zero. Only a single combination of these parameters can be determined from neutrino-trident production, so this example will study how well differential LHC measurements can help break the remaining degeneracy between Wilson coefficients that occurs given only the inclusive branching ratio measurement. For comparison we also fit to the inclusive LHC measurement. The results assuming differential LHC measurements are shown in Fig. 4. For comparison the result assuming only an inclusive branching ratio measurement with 3000 fb$^{-1}$ is shown as well. The improvement going from inclusive to differential measurements at the LHC is significant, with bounds on $C_{\substack{le \\ 2222}}$ improving from $\mathcal{O}(10)$ to $\mathcal{O}(1)$. This strong improvement is in large part due to the sign of the SMEFT deviations changing in different regions of $(\theta_1, \theta_2)$ space, which is partially averaged out in the inclusive analysis, while the differential analysis resolves the opposite-sign contributions. The flat direction in the $C_{\substack{le \\ 2222}}$ versus $C_{\substack{ll \\ 2222}}$ plane present with just neutrino trident production leads to the elongated shape of the constraint ellipse in this figure. This is removed by the high-luminosity LHC data.

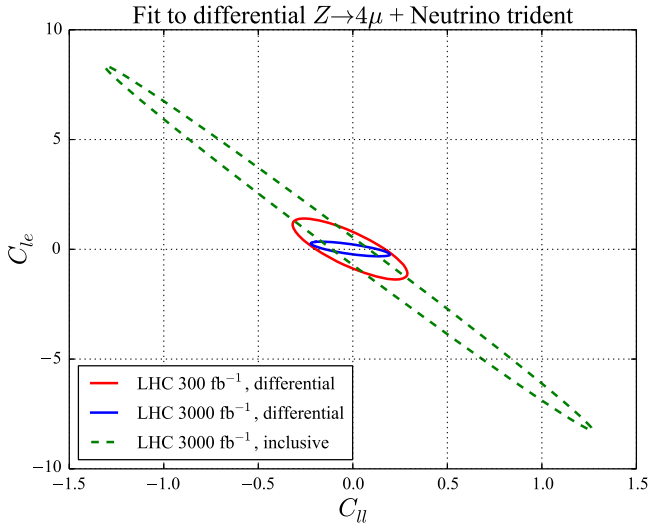


FIG. 4. 68% C.L. bounds on the combination of differential LHC $Z \to 4\mu$ data and neutrino trident production assuming nonzero $C_{\substack{ll \\ 2222}}$ and $C_{\substack{le \\ 2222}}$

## V. CONCLUSIONS

In this paper we have studied what can be learned about four-muon operators in the SMEFT from rare $Z \to 4\mu$ decays at the LHC. Measurements of this decay mode constrain linear combinations of Wilson coefficients not accessible in other processes. We determined the constraints imposed on these coefficients from current measurements of the inclusive branching ratio, and showed their complementarity with existing constraints from neutrino-trident production. Future differential measurements of $Z \to 4\mu$ have the potential to completely determine the four-muon Wilson coefficients in SMEFT. We show that strong bounds on all four-muon interactions can be obtained assuming 3000 fb$^{-1}$ of integrated luminosity at the LHC.

We have focused in this paper on the $Z \to 4\mu$ decay since experimental searches for this channel exist. However, measurements of the decay $Z \to 2\mu 2\tau$ would probe SMEFT Wilson coefficients such as $C_{\substack{ll\\2332}}$, $C_{\substack{le\\2332}}$, and $C_{\substack{ee\\2332}}$, while $Z \to 4\tau$ would probe $C_{\substack{ll\\3333}}$, $C_{\substack{le\\3333}}$, and $C_{\substack{ee\\3333}}$. Only $C_{\substack{le\\2332}}$ is weakly constrained by $\tau$-decays. The remaining coefficients are completely untested. The suggested rare $Z$-decays would provide the first tests of this unknown sector of the SMEFT. To our knowledge these rare $Z$-decays into $\tau$-leptons have not been considered. However, searches for Higgs bosons into these final states have been performed at the LHC [34,35]. We encourage the ATLAS and CMS collaborations to perform these searches with future data.

## ACKNOWLEDGMENTS

We thank W. Hopkins for helpful discussions. R. B. is supported by the DOE Contract No. DE-AC02-06CH11357. C.-Y. C. is supported by the NSF Grant No. NSF-1740142. F. P. and D. W. are supported by the DOE Grants No. DE-FG02-91ER40684 and No. DE-AC02-06CH11357.

## APPENDIX A: VERTEX SHIFTS

We present here the vertex shift factors. Our conventions for the $Zff$ vertices are such that

$$V^{\mu}_{\rm SMEFT} P_{L/R} = V^{\mu}_{\rm SM} P_{L/R} \left\{ 1 + \frac{v^2}{\Lambda^2} \delta g_V^{L/R} \right\}. \quad \text{(A1)}$$

The Higgs vev can be expressed in term of input parameters as

$$v^2 = \frac{1}{\sqrt{2} G_\mu}. \quad \text{(A2)}$$

The shift factors that appear in the dimension-6 corrections to the $Z \to 4\mu$ decay width in the $(G_\mu, M_W, M_Z)$ input scheme are

$$\begin{aligned}
\delta g_{\gamma l_i} &= \frac{1}{4 s_W^2} \left\{ \left( C_{\substack{ll\\1221}} + C_{\substack{ll\\2112}} - C^{(3)}_{\substack{\phi l\\11}} - C^{(3)}_{\substack{\phi l\\22}} \right) s_W^2 - C_{\phi D} c_W^2 - 4 c_W s_W C_{\phi WB} \right\}, \\
\delta g^L_{Z l_i} &= \frac{1}{4(1 - 2 s_W^2)} \left\{ \left( C_{\substack{ll\\1221}} + C_{\substack{ll\\2112}} - 2 C^{(3)}_{\substack{\phi l\\22}} \right)(1 - 2 s_W^2) + (1 + 2 c_W^2) C_{\phi D} + 8 c_W s_W C_{\phi WB} + 4 C^{(1)}_{\substack{\phi l\\ii}} + 2(1 + 2 s_W^2) C^{(3)}_{\substack{\phi l\\ii}} \right\}, \\
\delta g^R_{Z l_i} &= \frac{1}{4 s_W^2} \left\{ \left( C_{\substack{ll\\1221}} + C_{\substack{ll\\2112}} - 2 C^{(3)}_{\substack{\phi l\\11}} - 2 C^{(3)}_{\substack{\phi l\\22}} \right) s_W^2 - (1 + c_W^2) C_{\phi D} - 4 c_W s_W C_{\phi WB} - 2 C_{\substack{\phi e\\ii}} \right\}, \\
\delta g^L_{Z \nu_i} &= \frac{1}{4} \left\{ C_{\substack{ll\\1221}} + C_{\substack{ll\\2112}} - 2 C^{(3)}_{\substack{\phi l\\11}} - 2 C^{(3)}_{\substack{\phi l\\22}} - C_{\phi D} + 4 C^{(1)}_{\substack{\phi l\\ii}} - 4 C^{(3)}_{\substack{\phi l\\ii}} \right\}, \\
\delta g^L_{Z u_i} &= \frac{1}{4(4 s_W^2 - 3)} \left\{ (1 - 4 c_W^2) \left( C_{\substack{ll\\1221}} + C_{\substack{ll\\2112}} - 2 \left( C^{(3)}_{\substack{\phi l\\11}} + C^{(3)}_{\substack{\phi l\\22}} \right) \right) - (1 + 4 c_W^2) C_{\phi D} - 16 c_W s_W C_{\phi WB} + 12 C^{(1)}_{\substack{\phi q\\ii}} - 12 C^{(3)}_{\substack{\phi q\\ii}} \right\}, \\
\delta g^R_{Z u_i} &= \frac{1}{4 s_W^2} \left\{ s_W^2 \left( C_{\substack{ll\\1221}} + C_{\substack{ll\\2112}} - 2 \left( C^{(3)}_{\substack{\phi l\\11}} + C^{(3)}_{\substack{\phi l\\22}} \right) \right) - (1 + c_W^2) C_{\phi D} - 4 c_W s_W C_{\phi WB} + 3 C_{\substack{\phi u\\ii}} \right\}, \\
\delta g^L_{Z d_i} &= \frac{1}{4(1 + 2 c_W^2) s_W} \left\{ (1 + 2 c_W^2) \left( C_{\substack{ll\\1221}} + C_{\substack{ll\\2112}} - 2 \left( C^{(3)}_{\substack{\phi l\\11}} + C^{(3)}_{\substack{\phi q\\22}} \right) \right) s_W \right. \\
&\quad \left. + 8 c_W s_W^2 C_{\phi WB} + (2 c_W^2 - 1) s_W C_{\phi D} + 12 \left( C^{(1)}_{\substack{\phi q\\ii}} + C^{(3)}_{\substack{\phi q\\ii}} \right) s_W \right\}, \\
\delta g^R_{Z d_i} &= \frac{1}{4 s_W^2} \left\{ s_W^2 \left( C_{\substack{ll\\1221}} + C_{\substack{ll\\2112}} - 2 \left( C^{(3)}_{\substack{\phi l\\11}} + C^{(3)}_{\substack{\phi l\\22}} \right) \right) - (1 + c_W^2) C_{\phi D} - 4 c_W s_W C_{\phi WB} - 6 C_{\substack{\phi d\\ii}} \right\}, \\
\delta g^L_{W l_i} &= \frac{1}{4} \left\{ C_{\substack{ll\\1221}} + C_{\substack{ll\\2112}} - 2 C^{(3)}_{\substack{\phi l\\11}} - 2 C^{(3)}_{\substack{\phi l\\22}} + 4 C^{(3)}_{\substack{\phi l\\ii}} \right\}.
\end{aligned} \quad \text{(A3)}$$

We have made use of the on-shell definition of the weak mixing angle

$$s_W^2 = 1 - \frac{M_W^2}{M_Z^2} = 1 - c_W^2. \tag{A4}$$

## APPENDIX B: Z DECAY WIDTHS AT LEADING ORDER

We summarize here all leading-order SMEFT contributions to the $Z$-decay widths that have been used in this paper. Our conventions are such that

$$\Gamma^{\rm SMEFT}(Z \to f\bar{f}) = \Gamma^{\rm SM}_{f\bar{f}} + \frac{M_Z^2}{\Lambda^2}\delta\Gamma_{f\bar{f}} \tag{B1}$$

with the following analytic expressions for the SMEFT contributions:

$$\begin{aligned}
\delta\Gamma_{\nu_i\nu_i} &= \frac{M_Z}{12\pi}\delta g^L_{Z\nu_i},\\
\delta\Gamma_{l_il_i} &= \frac{M_Z}{12\pi}\{(1-2c_W^2)^2\delta g^L_{Zl_i} + 4s_W^4\delta g^R_{Zl_i}\},\\
\delta\Gamma_{u_iu_i} &= \frac{N_cM_Z}{108\pi}\{16s_W^4\delta g^R_{Zu_i} + (3-4s_W^2)^2\delta g^L_{Zu_i}\},\\
\delta\Gamma_{bb} &= \frac{N_cM_Z}{108\pi}\Big\{2s_W^2(2s_W^2 - \beta_b^2(9-4s_W^2))\delta g^R_{Zb} + (3-2s_W^2)(3-2s_W^2\\
&\quad - \beta_b^2(3+4s_W^2))\delta g^L_{Zb} - 9\sqrt{2}\beta_b(3-4s_W^2)\Big(s_W C_{\substack{dB\\33}} + c_W C_{\substack{dW\\33}}\Big)\Big\}\sqrt{1-4\beta_b^2}.
\end{aligned} \tag{B2}$$

We have assumed a nonvanishing bottom mass, appearing as

$$\beta_b = \frac{m_b}{M_Z}. \tag{B3}$$

The remaining two down-type partial widths can be found by setting $\beta_b = 0$ and appropriately changing the generational indices of the $\{3,3\}$ Wilson coefficients. We give below the numerical expressions for the SMEFT dependence of the decay width for the process $Z \to 4\mu$, obtained with MADGRAPH:

$$\begin{aligned}
\Gamma^{\rm LO}(Z\to 4\mu) = \Gamma^{\rm LO}_{\rm SM}(Z\to 4\mu) + \frac{v^2}{\Lambda^2}\Big\{&0.0260C_{\substack{le\\2222}} + 0.0711C_{\substack{ll\\2222}} + 0.0444C_{\substack{ee\\2222}}\\
&+ 15.0C_{\substack{ll\\1221}} + 24.0C_{\phi WB} + 6.08C_{\phi D} - 0.0062C^{(1)}_{\substack{\phi l\\11}} + 12.0C^{(1)}_{\substack{\phi l\\22}} - 2.14C^{(3)}_{\substack{\phi l\\11}}\\
&+ 0.445C^{(3)}_{\substack{\phi l\\22}} + 0.733C_{\substack{\phi e\\22}}\Big\}\times 10^{-6}\ \text{GeV}.
\end{aligned} \tag{B4}$$

For completeness we also give the result for the process $Z \to 2\mu 2e$ below:

$$\begin{aligned}
\Gamma^{\rm LO}(Z\to 2\mu 2e) = \Gamma^{\rm LO}_{\rm SM}(Z\to 2\mu 2e) + \frac{v^2}{\Lambda^2}\Big\{&29.9C_{\substack{ll\\1221}} + 0.0752C_{\substack{ll\\1212}} + 0.180C_{\substack{ee\\1122}}\\
&+ 0.0840C_{\substack{ee\\1212}} + 0.108C_{\substack{le\\1122}} + 0.0769C_{\substack{le\\1221}}\\
&+ 0.0740C_{\substack{le\\1212}} + 0.108C_{\substack{le\\2211}} + 46.9C_{\phi WB}\\
&+ 12.1C_{\phi D} + 12.1C^{(1)}_{\substack{\phi l\\11}} + 12.1C^{(1)}_{\substack{\phi l\\22}}\\
&- 1.50C^{(3)}_{\substack{\phi l\\11}} - 1.50C^{(3)}_{\substack{\phi l\\22}} + 0.927C_{\substack{\phi e\\11}}\\
&+ 0.921C_{\substack{\phi e\\22}}\Big\}\times 10^{-6}\ \text{GeV}.
\end{aligned} \tag{B5}$$

The leading-order SM results are

$$\Gamma^{\mathrm{LO}}_{\mathrm{SM}}(Z \to 4\mu) = 2.86 \times 10^{-6}\ \mathrm{GeV} \quad \text{and} \quad \Gamma^{\mathrm{LO}}_{\mathrm{SM}}(Z \to 2\mu 2e) = 5.62 \times 10^{-6}\ \mathrm{GeV}. \tag{B6}$$


[1] W. Buchmuller and D. Wyler, Nucl. Phys. **B268**, 621 (1986).
[2] C. Arzt, M. B. Einhorn, and J. Wudka, Nucl. Phys. **B433**, 41 (1995).
[3] B. Grzadkowski, M. Iskrzynski, M. Misiak, and J. Rosiek, J. High Energy Phys. 10 (2010) 085.
[4] Z. Han and W. Skiba, Phys. Rev. D **71**, 075009 (2005).
[5] A. Pomarol and F. Riva, J. High Energy Phys. 01 (2014) 151.
[6] C. Y. Chen, S. Dawson, and C. Zhang, Phys. Rev. D **89**, 015016 (2014).
[7] J. Ellis, V. Sanz, and T. You, J. High Energy Phys. 07 (2014) 036.
[8] J. D. Wells and Z. Zhang, Phys. Rev. D **90**, 033006 (2014).
[9] A. Falkowski and F. Riva, J. High Energy Phys. 02 (2015) 039.
[10] J. de Blas, M. Ciuchini, E. Franco, S. Mishima, M. Pierini, L. Reina, and L. Silvestrini, J. High Energy Phys. 12 (2016) 135.
[11] V. Cirigliano, W. Dekens, J. de Vries, and E. Mereghetti, Phys. Rev. D **94**, 034031 (2016).
[12] C. Hartmann, W. Shepherd, and M. Trott, J. High Energy Phys. 03 (2017) 060.
[13] A. Falkowski, M. Gonzlez-Alonso, and K. Mimouni, J. High Energy Phys. 08 (2017) 123.
[14] A. Biekoetter, T. Corbett, and T. Plehn, SciPost Phys. **6**, 064 (2019).
[15] C. Grojean, M. Montull, and M. Riembau, J. High Energy Phys. 03 (2019) 020.
[16] N. P. Hartland, F. Maltoni, E. R. Nocera, J. Rojo, E. Slade, E. Vryonidou, and C. Zhang, J. High Energy Phys. 04 (2019) 100.
[17] I. Brivio, S. Bruggisser, F. Maltoni, R. Moutafis, T. Plehn, E. Vryonidou, S. Westhoff, and C. Zhang, J. High Energy Phys. 02 (2020) 131.
[18] R. Aoude, T. Hurth, S. Renner, and W. Shepherd, J. High Energy Phys. 12 (2020) 113.
[19] R. Alonso, E. E. Jenkins, A. V. Manohar, and M. Trott, J. High Energy Phys. 04 (2014) 159.
[20] J. M. Cullen and B. D. Pecjak, J. High Energy Phys. 11 (2020) 079.
[21] W. Altmannshofer, C. Niehoff, P. Stangl, and D. M. Straub, Eur. Phys. J. C **77**, 377 (2017).
[22] R. Boughezal, F. Petriello, and D. Wiegand, Phys. Rev. D **101**, 116002 (2020).
[23] W. Altmannshofer, S. Gori, M. Pospelov, and I. Yavin, Phys. Rev. Lett. **113**, 091801 (2014).
[24] J. L. Rainbolt and M. Schmitt, Phys. Rev. D **99**, 013004 (2019).
[25] I. Brivio, Y. Jiang, and M. Trott, J. High Energy Phys. 12 (2017) 070.
[26] S. Dawson and P. P. Giardino, Phys. Rev. D **101**, 013001 (2020).
[27] S. Chatrchyan *et al.* (CMS Collaboration), J. High Energy Phys. 12 (2012) 034.
[28] V. Khachatryan *et al.* (CMS Collaboration), Phys. Lett. B **763**, 280 (2016).
[29] A. M. Sirunyan *et al.* (CMS Collaboration), Eur. Phys. J. C **78**, 165 (2018).
[30] G. Aad *et al.* (ATLAS Collaboration), Phys. Rev. Lett. **112**, 231806 (2014).
[31] S. R. Mishra *et al.* (CCFR Collaboration), Phys. Rev. Lett. **66**, 3117 (1991).
[32] D. Geiregat *et al.* (CHARM-II Collaboration), Phys. Lett. B **245**, 271 (1990).
[33] Y. Gao, A. V. Gritsan, Z. Guo, K. Melnikov, M. Schulze, and N. V. Tran, Phys. Rev. D **81**, 075022 (2010).
[34] V. Khachatryan *et al.* (CMS Collaboration), J. High Energy Phys. 01 (2016) 079.
[35] V. Khachatryan *et al.* (CMS Collaboration), J. High Energy Phys. 10 (2017) 076.